CrossMark

Influence of Magnetic Field on Qutrit Teleportation under Intrinsic Decoherence

Negar Naderi[1] · Mojtaba Jafapour[1]

Abstract
We study qutrit teleportation through a qutrit *xyz* chain, in the presence of intrinsic decoherence and a non-homogeneous magnetic field. We study the effects of intrinsic phase change, magnetic field and entanglement of the initial state of the channel. It is observed that while the intrinsic phase change and the non-homogeneity of the magnetic field have adverse effects on the teleportation fidelity, the entanglement of the initial state of the channeled enhances the latter. Moreover, the intrinsic decoherence may remove the ripples from the time curve that is delivered by the Schrödinger channel.

Keywords Qutrit · Teleportation · Intrinsic decoherence · Environmental decoherence, Entangled state · Product state · Fidelity, Homogeneous magnetic field, Inhomogeneous magnetic field

1 Introduction

Quantum entanglement, a non-classical property of the physical systems, has been considered a resource to perform several information processing tasks which are not possible in the classical realm [1]. There has been a concerted effort to study the entanglement properties of the spin chains in the last decade; they have been used in several quantum information processes including quantum computations [2, 3], quantum communications [4] and have been considered as relatively realistic models to study quantum dots [5, 6], superconductivity [7] and phase transitions [8]. Spin chains, specifically the spin-$\frac{1}{2}$ ones, have been also considered as appropriate media to perform quantum teleportation and their properties in the absence [9–12] or in the presence of the environment decoherence [13–16]. A few papers also consider the effect of the intrinsic decoherence, as was formulated by Milburn [17], on teleportation via the $\frac{1}{2}$-spin chains

✉ Negar Naderi
  ghoroob_naderi@yahoo.com

  Mojtaba Jafapour
  mojtaba_jafarpour@hotmail.com

[1] Physics Department, Shahid Chamran University, Ahvaz, Iran

[13, 18]. It has been also reported that application of a homogeneous magnetic field may reduce the adverse effect of the intrinsic decoherence on the teleportation [13], while another research reports a similar effect, in a *xxz* chain, if a non-homogeneous magnetic field is applied [18].

Reports regarding qutrit teleportation are few and far between [19–21]. A reference reports qutrit state transfer between two cavities [19]. Probabilistic qutrit teleportation has been also discussed [20]. Teleportation of one – and two-qutrit systems, through a maximally entangled quantum channel of three-qutrit channel, has been also reported [21]. We have also considered the teleportation of a qutrit state through an xyz chain model, and have studied the effect of the entanglement of the initial state of the channel on that, previously [22]. Our aim in this work is to consider qutrit teleportation through a qutrit *xyz* chain, in the presence of the intrinsic decoherence; while a non-homogeneous magnetic field is also applied, to study its possible improving effects onthe teleportation, as has been reported in the case of spin-$\frac{1}{2}$ models [18].

2 Theoretical Model

We intend to study qutrit teleportation through a qutrit*xyz*Heisenberg chain under non-homogeneous magnetic field. Considering a two-qutrit chain, its Hamiltonian is given by

$$H = J_X S_1^X \otimes S_2^X + J_Y S_1^Y \otimes S_2^Y + J_Z S_1^Z \otimes S_2^Z + (B+b)(S_1^Z \otimes I) + (B-b)(I \otimes S_2^Z), \quad (1)$$

Where, J_i's are the interaction parameters, B is homogeneous magnetic field, b is the inhomogeneous magnetic field and the qutrit operators are given by [23].

$$S^x = \frac{1}{\sqrt{2}} \begin{pmatrix} 0 & 1 & 0 \\ 1 & 0 & 1 \\ 0 & 1 & 0 \end{pmatrix}, \qquad (2-a)$$

$$S^y = \frac{1}{\sqrt{2}} \begin{pmatrix} 0 & -i & 0 \\ i & 0 & -i \\ 0 & i & 0 \end{pmatrix}, \qquad (2-b)$$

$$S^z = \begin{pmatrix} 1 & 0 & 0 \\ 0 & 0 & 0 \\ 0 & 0 & -1 \end{pmatrix}. \qquad (2-c)$$

The matrix representation of the Hamiltonian in the computational basis is given by

$$H = \begin{pmatrix} 2+2B & 0 & 0 & 0 & -1 & 0 & 0 & 0 & 0 \\ 0 & B+b & 0 & 2 & 0 & -1 & 0 & 0 & 0 \\ 0 & 0 & -2+2b & 0 & 2 & 0 & 0 & 0 & 0 \\ 0 & 2 & 0 & -b+B & 0 & 0 & 0 & -1 & 0 \\ -1 & 0 & 2 & 0 & 0 & 0 & 2 & 0 & -1 \\ 0 & -1 & 0 & 0 & 0 & b-B & 0 & 2 & 0 \\ 0 & 0 & 0 & 0 & 2 & 0 & -2-2b & 0 & 0 \\ 0 & 0 & 0 & -1 & 0 & 2 & 0 & -b-B & 0 \\ 0 & 0 & 0 & 0 & -1 & 0 & 0 & 0 & 2-2B \end{pmatrix}, (3)$$

whose eigenvalues are expressed by

$$E_1 = -\left(5 + b^2 + B^2 - 2A_1\right)^{\frac{1}{2}}, \qquad (4-a)$$

$$E_2 = -E_1, \qquad (4-b)$$

$$E_3 = -\left(5 + b^2 + B^2 + 2A_1\right)^{\frac{1}{2}}, \qquad (4-c)$$

$$E_4 = -E_3, \qquad (4-d)$$

$$E_5 = Root_1\Big[-48 - 16b^2 + 64B^2 + \left(56 - 8b^2 + 16B^2 + 16b^2B^2\right)X$$
$$+\left(12 + 16b^2 - 16B^2\right)X^2 + \left(-18 - 4b^2 - 4B^2\right)X^3 + X^5 = 0\Big], \qquad (4-e)$$

$$E_6 = Root_2\Big[-48 - 16b^2 + 64B^2 + \left(56 - 8b^2 + 16B^2 + 16b^2B^2\right)X$$
$$+\left(12 + 16b^2 - 16B^2\right)X^2 + \left(-18 - 4b^2 - 4B^2\right)X^3 + X^5 = 0\Big], \qquad (4-f)$$

$$E_7 = Root_3\Big[-48 - 16b^2 + 64B^2 + \left(56 - 8b^2 + 16B^2 + 16b^2B^2\right)X$$
$$+\left(12 + 16b^2 - 16B^2\right)X^2 + \left(-18 - 4b^2 - 4B^2\right)X^3 + X^5 = 0\Big], \qquad (4-g)$$

$$E_8 = Root_4\Big[-48 - 16b^2 + 64B^2 + \left(56 - 8b^2 + 16B^2 + 16b^2B^2\right)X$$
$$+\left(12 + 16b^2 - 16B^2\right)X^2 + \left(-18 - 4b^2 - 4B^2\right)X^3 + X^5 = 0\Big], \qquad (4-h)$$

$$E_9 = Root_5\Big[-48 - 16b^2 + 64B^2 + \left(56 - 8b^2 + 16B^2 + 16b^2B^2\right)X$$
$$+\left(12 + 16b^2 - 16B^2\right)X^2 + \left(-18 - 4b^2 - 4B^2\right)X^3 + X^5 = 0\Big]. \qquad (4-i)$$

And the corresponding eigenfunctions are

$$|\psi_1\rangle = \Big\{\left(1 - A_1^* + B^*(B^* - E_2^*)\right)|1_{\hat{1}}, 0_{\hat{2}}\rangle + E_2^*\Big(2 + A_2^*\left(-B^* + (b + E_2)^*\right)\Big)|0_{\hat{1}}, 1_{\hat{2}}\rangle$$
$$+A_2^* E_2^*|1_{\hat{1}}, 2_{\hat{2}}\rangle + E_2^*|2_{\hat{1}}, 1_{\hat{2}}\rangle\Big\}\Big(1 + |A_2|^2 + |(1 - A_1 + B(B - E_2))|^2\left(|E_2|^2\right)^{-1}$$
$$+|(2 + A_2(b - B + E_2))|^2\Big)^{-\frac{1}{2}}, \qquad (5-a)$$

$$|\psi_2\rangle = \left\{\left(-1 + (A_1 - B(B + E_2))^*\right)|1_{\hat{1}}, 0_{\hat{2}}\rangle + E_2^*\left(2 + A_3^*\left(b^* - (B + E_2)^*\right)\right)|0_{\hat{1}}, 1_{\hat{2}}\rangle \right.$$
$$+ A_3^* E_2^*|1_{\hat{1}}, 2_{\hat{2}}\rangle + E_2^*|2_{\hat{1}}, 1_{\hat{2}}\rangle\right\}\left(1 + |A_3|^2 + |(-1 + A_1 - B(B + E_2))|^2 \left(|E_2|^2\right)^{-1}\right. \qquad (5-b)$$
$$\left. + |(2 + A_3(b - B + E_2))|^2\right)^{-\frac{1}{2}},$$

$$|\psi_3\rangle = \left\{\left(1 + (A_1 + B(B - E_4))^*\right)|1_{\hat{1}}, 0_{\hat{2}}\rangle + E_4^*\left(2 + A_4^*\left(-B^* + (b + E_4)^*\right)\right)|0_{\hat{1}}, 1_{\hat{2}}\rangle \right.$$
$$+ A_4^* E_4^*|1_{\hat{1}}, 2_{\hat{2}}\rangle + E_4^*|2_{\hat{1}}, 1_{\hat{2}}\rangle\right\}\left(1 + |A_4|^2 + |(1 + A_1 + B(B - E_4))|^2 \left(|E_4|^2\right)^{-1}\right.$$
$$\left. + |(2 + A_4(b - B + E_4))|^2\right)^{-\frac{1}{2}},$$
$$(5-c)$$

$$|\psi_4\rangle = \left\{-\left(1 + A_1^* + (B(B + E_4))^*\right)|1_{\hat{1}}, 0_{\hat{2}}\rangle + E_4^*\left(2 + A_5^*\left(b^* - (B + E_4)^*\right)\right)|0_{\hat{1}}, 1_{\hat{2}}\rangle \right.$$
$$+ A_5^* E_4^*|1_{\hat{1}}, 2_{\hat{2}}\rangle + E_4^*|2_{\hat{1}}, 1_{\hat{2}}\rangle\right\}\left(1 + |A_5|^2 + |(1 + A_1 + B(B + E_4))|^2 \left(|E_4|^2\right)^{-1}\right.$$
$$\left. + |(2 - A_5(-b + B + E_4))|^2\right)^{-\frac{1}{2}},$$
$$(5-d)$$

$$|\psi_5\rangle = \left\{\left(-9 - 2A_6^* + 2A_7^* + 2(B^* - 1)E_5^* + (E_5^*)^2\right)|0_{\hat{1}}, 0_{\hat{2}}\rangle + (-2 - A_6^*)|0_{\hat{1}}, 2_{\hat{2}}\rangle \right.$$
$$\left. + (2 - 2B^* - E_5^*)|1_{\hat{1}}, 1_{\hat{2}}\rangle + (-2 + A_7^*)|2_{\hat{1}}, 0_{\hat{2}}\rangle + |2_{\hat{1}}, 2_{\hat{2}}\rangle\right\}$$
$$\left(1 + |-2 - A_6|^2 + |-2 + A_7|^2 + |2 - 2B - E_5|^2 + |-9 - 2A_6 + 2A_7 + 2(B-1)E_5 + (E_5)^2|^2\right)^{-\frac{1}{2}},$$
$$(5-e)$$

$$|\psi_6\rangle = \left\{\left(-9 - 2A_8^* + 2A_9^* + 2(B^* - 1)E_6^* + (E_6^*)^2\right)|0_{\hat{1}}, 0_{\hat{2}}\rangle + (-2 - A_8^*)|0_{\hat{1}}, 2_{\hat{2}}\rangle \right.$$
$$\left. + (2 - 2B^* - E_6^*)|1_{\hat{1}}, 1_{\hat{2}}\rangle + (-2 + A_9^*)|2_{\hat{1}}, 0_{\hat{2}}\rangle + |2_{\hat{1}}, 2_{\hat{2}}\rangle\right\}$$
$$\left(1 + |-2 - A_8|^2 + |-2 + A_9|^2 + |2 - 2B - E_6|^2 + |-9 - 2A_8 + 2A_9 + 2(B-1)E_6 + (E_6)^2|^2\right)^{-\frac{1}{2}},$$
$$(5-f)$$

$$|\psi_7\rangle = \left\{\left(-9 - 2A_{10}^* + 2A_{11}^* + 2(B^* - 1)E_7^* + (E_7^*)^2\right)|0_{\hat{1}}, 0_{\hat{2}}\rangle + (-2 - A_{10}^*)|0_{\hat{1}}, 2_{\hat{2}}\rangle \right.$$
$$\left. + (2 - 2B^* - E_7^*)|1_{\hat{1}}, 1_{\hat{2}}\rangle + (-2 + A_{11}^*)|2_{\hat{1}}, 0_{\hat{2}}\rangle + |2_{\hat{1}}, 2_{\hat{2}}\rangle\right\}$$
$$\left(1 + |-2 - A_{10}|^2 + |-2 + A_{11}|^2 + |2 - 2B - E_7|^2 + |-9 - 2A_{10} + 2A_{11} + 2(B-1)E_7 + (E_7)^2|^2\right)^{-\frac{1}{2}},$$
$$(5-g)$$

$$|\psi_8\rangle = \left\{\left(-9 - 2A_{12}^* + 2A_{13}^* + 2(B^* - 1)E_8^* + (E_8^*)^2\right)|0_{\hat{1}}, 0_{\hat{2}}\rangle + (-2 - A_{12}^*)|0_{\hat{1}}, 2_{\hat{2}}\rangle \right.$$
$$\left. + (2 - 2B^* - E_8^*)|1_{\hat{1}}, 1_{\hat{2}}\rangle + (-2 + A_{13}^*)|2_{\hat{1}}, 0_{\hat{2}}\rangle + |2_{\hat{1}}, 2_{\hat{2}}\rangle\right\}$$
$$\left(1 + |-2 - A_{12}|^2 + |-2 + A_{13}|^2 + |2 - 2B - E_8|^2 + |-9 - 2A_{12} + 2A_{13} + 2(B-1)E_8 + (E_8)^2|^2\right)^{-\frac{1}{2}},$$
$$(5-h)$$

$$|\psi_9\rangle = \left\{ \left(-9 - 2A_{14}^* + 2A_{15}^* + 2(B^*-1)E_9^* + (E_9^*)^2\right)|0_{\hat{1}}, 0_{\hat{2}}\rangle + \left(-2 - A_{14}^*\right)|0_{\hat{1}}, 2_{\hat{2}}\rangle \right.$$
$$\left. + \left(2 - 2B^* - E_9^*\right)|1_{\hat{1}}, 1_{\hat{2}}\rangle + \left(-2 + A_{15}^*\right)|2_{\hat{1}}, 0_{\hat{2}}\rangle + |2_{\hat{1}}, 2_{\hat{2}}\rangle \right\}$$
$$\left(1 + |-2 - A_{14}|^2 + |-2 + A_{15}|^2 + |2 - 2B - E_9|^2 + \left|-9 - 2A_{14} + 2A_{15} + 2(B-1)E_9 + (E_9)^2\right|^2\right)^{-\frac{1}{2}},$$

$$(5-i)$$

Where, we have defined

$$A_1 = \left((4+b^2)(1+B^2)\right)^{\frac{1}{2}}. \tag{6-a}$$

$$A_2 = (A_1 - 4 + b(E_2 - b))(2E_2)^{-1}, \tag{6-b}$$

$$A_3 = (-A_1 + 4 + b(E_2 + b))(2E_2)^{-1}, \tag{6-c}$$

$$A_4 = (-A_1 - 4 + b(E_4 - b))(2E_4)^{-1}, \tag{6-d}$$

$$A_5 = (A_1 + 4 + b(E_4 + b))(2E_4)^{-1}, \tag{6-f}$$

$$A_6 = 4(-2 + b + B)(2 - 2b + E_5)^{-1}, \tag{6-f}$$

$$A_7 = 4(2 + b - B)(2 + 2b + E_5)^{-1}, \tag{6-g}$$

$$A_8 = 4(-2 + b + B)(2 - 2b + E_6)^{-1}, \tag{6-h}$$

$$A_9 = 4(2 + b - B)(2 + 2b + E_6)^{-1}, \tag{6-i}$$

$$A_{10} = 4(-2 + b + B)(2 - 2b + E_7)^{-1}, \tag{6-j}$$

$$A_{11} = 4(2 + b - B)(2 + 2b + E_7)^{-1}, \tag{6-k}$$

$$A_{12} = 4(-2 + b + B)(2 - 2b + E_8)^{-1}, \tag{6-l}$$

$$A_{13} = 4(2 + b - B)(2 + 2b + E_8)^{-1}, \tag{6-m}$$

$$A_{14} = 4(-2 + b + B)(2 - 2b + E_9)^{-1}, \qquad (6-n)$$

$$A_{15} = 4(2 + b - B)(2 + 2b + E_9)^{-1}, \qquad (6-o)$$

3 Schrödinger and Milburn Evolution of an Initial Product State

The evolution under Schrödinger equation is given by

$$\rho_{Sh}(t) = U(t)\rho(0)U^{\dagger}(t) \qquad (7)$$

where,

$$U(t) = e^{-i\frac{H(t-t_0)}{\hbar}}. \qquad (8)$$

The evolution of the initial state under Millburn model is given by

$$\frac{d\hat{\rho}(t)}{dt} = \frac{1}{\eta}\left\{ \left(e^{\frac{-i\eta\hat{H}}{\hbar}}\hat{\rho}(0)e^{\frac{i\eta\hat{H}}{\hbar}} \right) - \hat{\rho}(0) \right\}, \qquad (9)$$

where, η aris the minimum phase change and $\rho(0)$ the initial density matrix of the system [17]. Solving this equation we find [24].

$$\hat{\rho}(t)_M = \sum_{mn} \exp\left[\frac{-t\eta}{2}(E_m - E_n)^2 - it(E_m - E_n)\right]\langle\psi_m|\hat{\rho}(0)|\psi_n\rangle|\psi_m\rangle\langle\psi_n|. \qquad (10)$$

where, $|\psi_n\rangle$ and E_n are given in eqs. (5-a) to (5-i) and (4-a) to (4-i) respectively. Now considering the initial product state

$$|\psi_0\rangle = |0_1, 1_2\rangle. \qquad (11)$$

The matrix representation is given by

$$\rho_{Sh-P}(t) = \begin{pmatrix} 0 & 0 & 0 & 0 & 0 & 0 & 0 & 0 & 0 \\ 0 & |I_1|^2 & 0 & I_2I_1^* & 0 & I_3I_1^* & 0 & I_4I_1^* & 0 \\ 0 & 0 & 0 & 0 & 0 & 0 & 0 & 0 & 0 \\ 0 & I_1I_2^* & 0 & |I_2|^2 & 0 & I_3I_2^* & 0 & I_4I_2^* & 0 \\ 0 & 0 & 0 & 0 & 0 & 0 & 0 & 0 & 0 \\ 0 & I_1I_3^* & 0 & I_2I_3^* & 0 & |I_3|^2 & 0 & I_4I_3^* & 0 \\ 0 & 0 & 0 & 0 & 0 & 0 & 0 & 0 & 0 \\ 0 & I_1I_4^* & 0 & I_2I_4^* & 0 & I_3I_4^* & 0 & |I_4|^2 & 0 \\ 0 & 0 & 0 & 0 & 0 & 0 & 0 & 0 & 0 \end{pmatrix}, \qquad (12)$$

where, the I_i parameters are too complicated to write it down and they are saved in our computer program. Similarly, we find

$$\rho_{M-P} = \begin{pmatrix} 0 & 0 & 0 & 0 & 0 & 0 & 0 & 0 & 0 \\ 0 & H_1 & 0 & H_2 & 0 & H_3 & 0 & H_4 & 0 \\ 0 & 0 & 0 & 0 & 0 & 0 & 0 & 0 & 0 \\ 0 & H_5 & 0 & H_6 & 0 & H_7 & 0 & H_8 & 0 \\ 0 & 0 & 0 & 0 & 0 & 0 & 0 & 0 & 0 \\ 0 & H_9 & 0 & H_{10} & 0 & H_{11} & 0 & H_{12} & 0 \\ 0 & 0 & 0 & 0 & 0 & 0 & 0 & 0 & 0 \\ 0 & H_{13} & 0 & H_{14} & 0 & H_{15} & 0 & H_{16} & 0 \\ 0 & 0 & 0 & 0 & 0 & 0 & 0 & 0 & 0 \end{pmatrix}, \tag{13}$$

where, the H_i parameters are too complicated to write it down and they are saved in our computer program.

4 Teleportation using Schrödinger and Milburn Channel Whose Initial State is a Product One

We consider the following incoming state to be teleported

$$|\Lambda_{in}\rangle = \frac{1}{\sqrt{3}} \left(|0\rangle + |1\rangle + |2\rangle \right), \tag{14}$$

whose corresponding density matrix is expressed by

$$\rho_{in} = \frac{1}{3} \begin{pmatrix} 1 & 1 & 1 \\ 1 & 1 & 1 \\ 1 & 1 & 1 \end{pmatrix}. \tag{15}$$

The outgoing state is given by [25].

$$\rho_{out} = \sum_{j=0}^{8} Tr\left(E^j \rho(t)\right) \left\{ \Gamma^j \rho_{in} \Gamma^j \right\}, \tag{16}$$

where, $\Gamma^j (j = 1, ..., 8)$ are Gell-Mann matrices [26] and the density matrices E^j's represent the two-qutrit maximally entangled states (ME) [27] which are expressed in appendix 1 and 2, respectively.
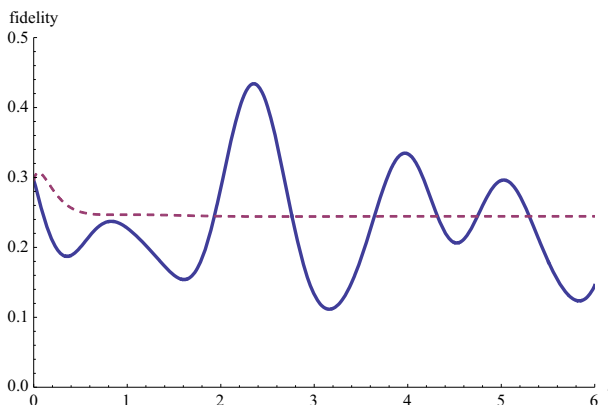

Fig. 1 F_{Sh-P} (solid line) and F_{M-P} (dotted line) as a function of t; $J_x = 1$, $J_y = 3$, $J_z = 2$, $b = 1$, $\eta = 1$, $B = 1$

The fidelity of the teleportation may be defined by [28].

$$F(\rho_{in}, \rho_{out}) = \left[Tr \left(\rho_{in}^{\frac{1}{2}} \rho_{out} \rho_{in}^{\frac{1}{2}} \right)^{\frac{1}{2}} \right]^2. \tag{17}$$

Now using eqs. (11), (14) and (15) we find

$$F_{Sh-P} = \frac{2}{27} \left[\left(4I_1 + \left(1 - 3^{\frac{1}{2}}i \right) I_2 \right) I_1^* + \left(\left(1 + 3^{\frac{1}{2}}i \right) I_1 + 4I_2 \right) I_2^* \right] \tag{18}$$

and using eqs. (12), (14) and (15) also we find

$$F_{M-P} = \frac{2}{27} \left(3^{\frac{1}{2}}(Im[H_2] - Im[H_5]) + Re[4H_1 + H_2 + H_5 + 4H_6] \right). \tag{19}$$

In Fig. 1, fidelities of Schrödinger and Milburn non-entangled channels as a function of time are plotted: It is observed that both start at the same value, but F_{M-P} decreases monotonically while F_{Sh-P} fluctuates in time. Moreover, it is observed that at specific periods of time, F_{Sh-P} gains larges values than that of Milburn fidelity and it is vice versa in specific periods of time.

Figure 2, depicts the fidelity of Schrödinger non-entangled channel as a function of time in the presence of an inhomogeneous magnetic field (b). By increasing an inhomogeneous magnetic field, the time periods of the fidelity become shorter and the latter decreases. Also, in Fig. 3, the fidelity of the Schrödinger non-entangled channel as a function of time for three different values of homogeneous magnetic field (B) is plotted. Increasing the homogeneous magnetic field, does not have any appreciable effect on the fidelity; only the latter increases slightly.
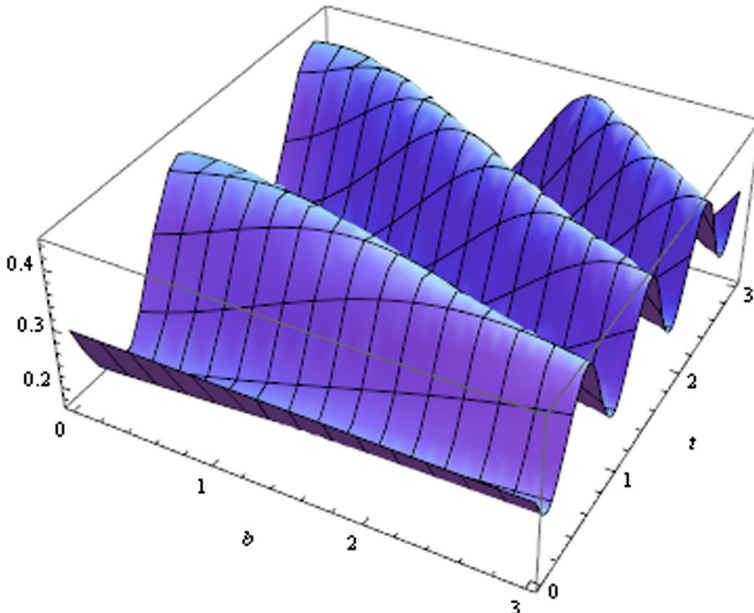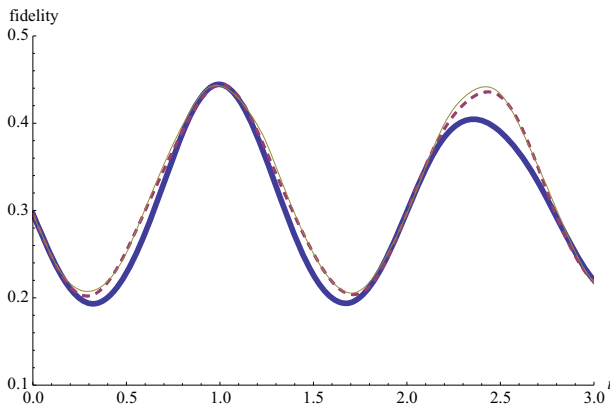

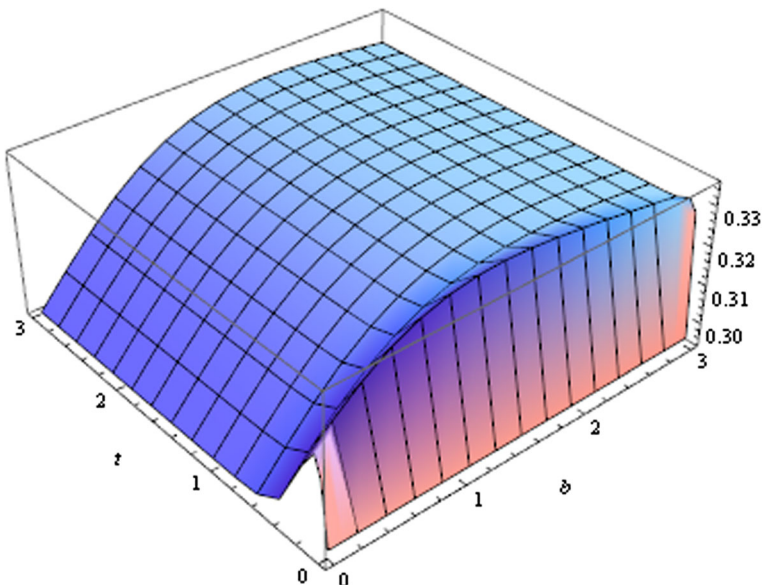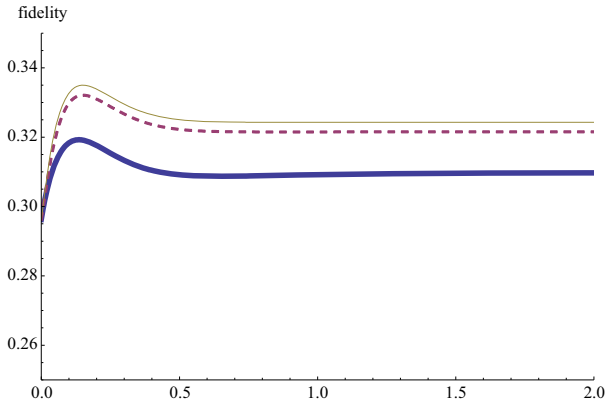**Fig. 2** F_{Sh-P} as a function of t and b; $J_x = 1$, $J_y = 3$, $J_z = 2$, $B = 10$

Fig. 3 F_{Sh-P} ($B = 3$: thick solid line, $B = 6$: dotted line, $B = 10$: thin solid line) as a function of t; $J_x = 1, J_y = 3, J_z = 2$, $b = 1$, $\eta = 1$

In Fig. 4 we have plotted fidelity of the non-entangled Milburn channel as a function of time and the inhomogeneous magnetic field (b). Also Fig. 5, depicts the fidelity of the non-entangled Milburn channel as a function of time, for three different values of homogeneous magnetic field (B). It is deduced that fidelity increases as the homogenous or the inhomogeneous magnetic field are increased.

In Fig. 6, the fidelity of non-entangled Milburn channel is shown as a function of time for three different values of the decoherence phase (η). It is observed that by increasing (η), the fidelity first decreases slightly but finally follows a plateau in time.

**Fig. 4** F_{M-P} as a function of t and b; $J_x = 1$, $J_y = 3$, $J_z = 2$, $\eta = 1$, $B = 10$

Fig. 5 F_{M-P} ($B = 3$: thick solid line, $B = 6$: dotted line, $B = 10$: thin solid line) as a function of t; $J_x = 1$, $J_y = 3$, $J_z = 2$, $b = 1$, $\eta = 1$

5 Teleportation using Schrödinger and Milburn Channel Whose Initial State is Entangled
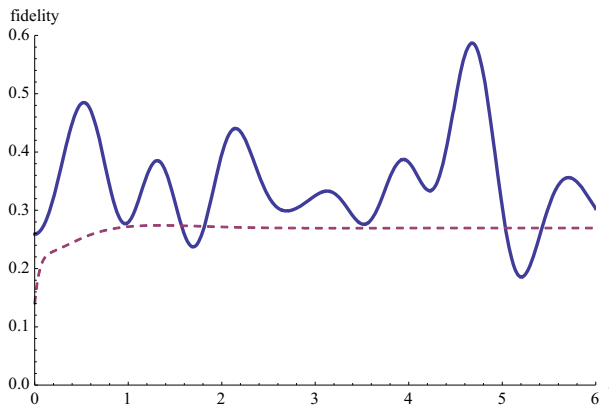
Now we consider the entangled state

$$|\phi^0\rangle = \frac{1}{\sqrt{3}} \left(|0, 0\rangle + |1, 1\rangle + |2, 2\rangle \right), \tag{20}$$

Which following the same procedure as the previous section leads to the following density matrices for the channel
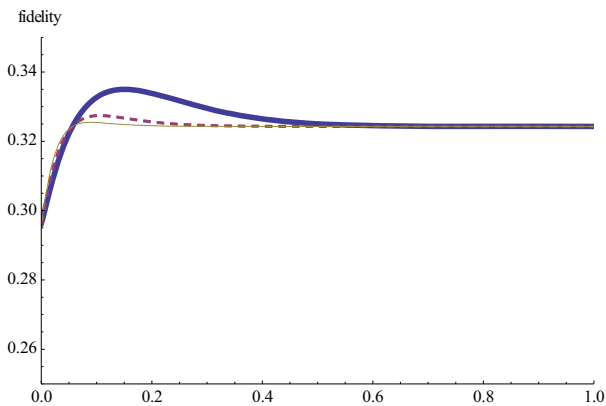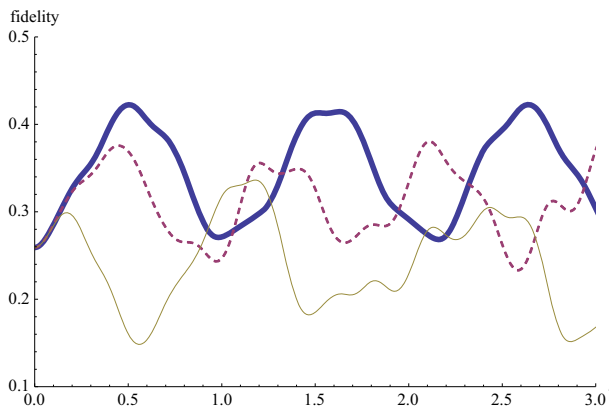

Fig. 6 F_{M-P} ($\eta = 1$: thick solid line, $\eta = 2$: dotted line, $\eta = 3$: thin solid line) as a function of t; $J_x = 1$, $J_y = 3$, $J_z = 2$, $b = 1$, $B = 10$

Fig. 7 F_{Sh-E} (solid line) and F_{M-E} (dotted line) as a function of t; $J_x = 1$, $J_y = 3$, $J_z = 2$, $b = 1$, $\eta = 1$, $B = 1$

$$\rho_{Sh-E}(t) = \begin{pmatrix} C_1 C_1^* & 0 & C_2 C_1^* & 0 & C_3 C_1^* & 0 & C_4 C_1^* & 0 & C_5 C_1^* \\ 0 & 0 & 0 & 0 & 0 & 0 & 0 & 0 & 0 \\ C_1 C_2^* & 0 & C_2 C_2^* & 0 & C_3 C_2^* & 0 & C_4 C_2^* & 0 & C_5 C_2^* \\ 0 & 0 & 0 & 0 & 0 & 0 & 0 & 0 & 0 \\ C_1 C_3^* & 0 & C_2 C_3^* & 0 & C_3 C_3^* & 0 & C_4 C_3^* & 0 & C_5 C_3^* \\ 0 & 0 & 0 & 0 & 0 & 0 & 0 & 0 & 0 \\ C_1 C_4^* & 0 & C_2 C_4^* & 0 & C_3 C_4^* & 0 & C_4 C_4^* & 0 & C_5 C_4^* \\ 0 & 0 & 0 & 0 & 0 & 0 & 0 & 0 & 0 \\ C_1 C_5^* & 0 & C_2 C_5^* & 0 & C_3 C_5^* & 0 & C_4 C_5^* & 0 & C_5 C_5^* \end{pmatrix}, \qquad (21)$$

where, the C_i parameters are too complicated to write it down and they are saved in our computer program, and

Fig. 8 F_{Sh-E} ($b = 0$: thick solid line, $b = 1$: dotted line, $b = 3$: thin solid line) as a function of t; $J_x = 1$, $J_y = 3$, $J_z = 2$, $B = 10$

$$\rho_{M-E} = \begin{pmatrix} G_1 & 0 & G_2 & 0 & G_3 & 0 & G_4 & 0 & G_5 \\ 0 & 0 & 0 & 0 & 0 & 0 & 0 & 0 & 0 \\ G_6 & 0 & G_7 & 0 & G_8 & 0 & G_9 & 0 & G_{10} \\ 0 & 0 & 0 & 0 & 0 & 0 & 0 & 0 & 0 \\ G_{11} & 0 & G_{12} & 0 & G_{13} & 0 & G_{14} & 0 & G_{15} \\ 0 & 0 & 0 & 0 & 0 & 0 & 0 & 0 & 0 \\ G_{16} & 0 & G_{17} & 0 & G_{18} & 0 & G_{19} & 0 & G_{20} \\ 0 & 0 & 0 & 0 & 0 & 0 & 0 & 0 & 0 \\ G_{21} & 0 & G_{22} & 0 & G_{23} & 0 & G_{24} & 0 & G_{25} \end{pmatrix}, \tag{22}$$

where, the G_i parameters are too complicated to write it down and they are saved in our computer program. The above two density matrices also lead to the following fidelities, following the same procedure as the previous section.

$$F_{Sh-E} = \frac{1}{27} \left(2*3^{\frac{1}{2}}Im\left[(C_3-C_2)C_4^*\right] + Re\left[\left(13C_2 + \left(7+2*3^{\frac{1}{2}}i\right)C_3 + \left(7-2*3^{\frac{1}{2}}i\right)C_4\right)C_2^* \right. \right.$$
$$\left. \left. + \left(\left(7-2*3^{\frac{1}{2}}i\right)C_2 + 13C_3 + \left(7+2*3^{\frac{1}{2}}i\right)C_4\right)C_3^* + (7(C_2+C_3)+13C_4)C_4^* + 8|C_5|^2\right] \right).$$

And   (23)

$$F_{M-E} = \frac{1}{27} \left(2*3^{\frac{1}{2}}Im[G_{12}-G_{14}-G_{17}+G_{18}-G_8+G_9] \right.$$
$$\left. + Re[13(G_7+G_{13}+G_{19}) + 7(G_8+G_9+G_{12}+G_{14}+G_{17}+G_{18}) + 8G_{25}] \right). \tag{24}$$

In Fig. 7, fidelity of the entangled Schrödinger and Milburn channel as a function of time are plotted. It is noted that the Schrödinger fidelity is larger than the Milburn one most of the time.

In Figs. 8 and 9, fidelities of entangled Schrödinger channel as a function of time for three different values of inhomogeneous (b) and homogeneous (B) magnetic fields are plotted. It is observed that as the inhomogeneous (b) and homogeneous (B) magnetic fields are increased, fidelities on the average decrease.

In Figs. 10 and 11, fidelities of the entangled Milburn channel as a function of time for three different values of the inhomogeneous (b) and the homogeneous (B) magnetic fields are shown. As the inhomogeneous magnetic field increases, the fidelity decreases; while, as the
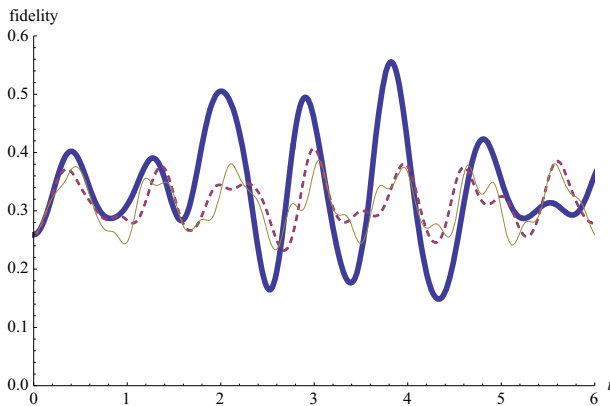
Fig. 9 F_{Sh-E} ($B=3$: thick solid line, $B=6$: dotted line, $B=10$: thin solid line) as a function of t; $J_x=1$, $J_y=3$, $J_z=2$, $b=1$
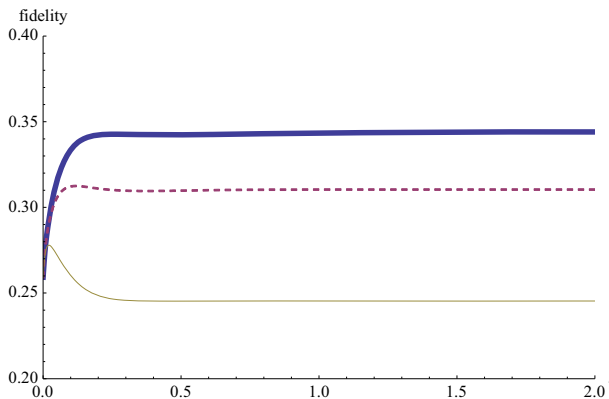
Fig. 10 F_{M-E} ($b = 0.1$: thick solid line, $b = 1$: dotted line, $b = 3$: thin solid line) as a function of t; $J_x = 1, J_y = 3$, $J_z = 2$, $\eta = 1$, $B = 10$

homogeneous magnetic field increases the fidelity is increased. Moreover, for large values of the homogeneous field, fidelity follows a plateau.

In Fig. 12, fidelity of entangled Milburn channel as a function of time for three different values of decoherence phase (η) are shown. It is observed that, when the channel is entangled, an increase in (η), initially increases the fidelity slightly for small periods of time; however, does not have an appreciable effect for large times.

6 Comparison of the Fidelity for Entangled and Non-Entangled Channels Under the Schrödinger and Milburn Evolution

In Fig. 13, F_{Sh-P} and F_{Sh-E} and in Fig. 14 F_{M-P} and F_{M-E} as a function of time are shown. In both of Schrödinger and Milburn evolution, fidelity of entangled channel is superior to non-entangled channel in most of the times. However, for small times, the situation is vice versa.
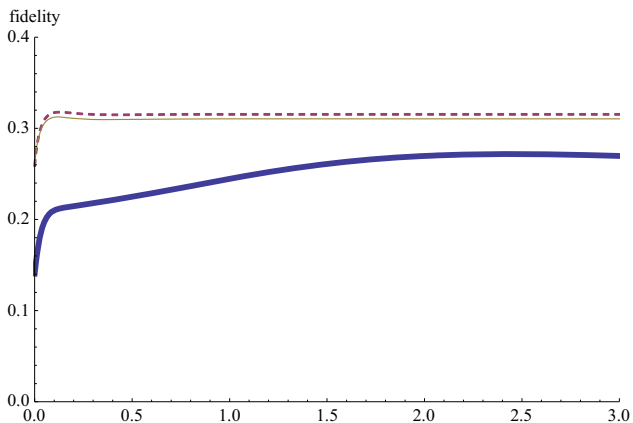
Fig. 11 F_{M-E} ($B = 3$: thick solid line, $B = 6$: dotted line, $B = 10$: thin solid line) as a function of t; $J_x = 1, J_y = 3$, $J_z = 2$, $b = 1$, $\eta = 1$
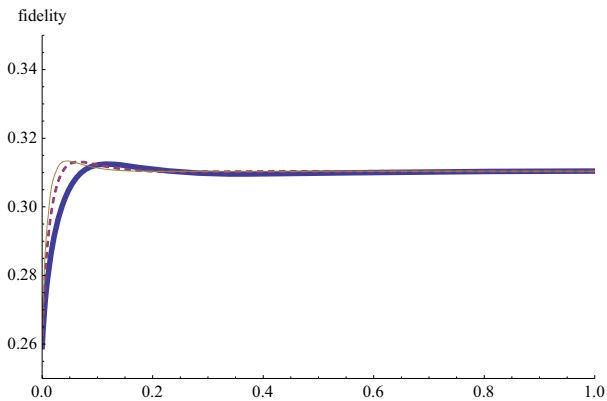
Fig. 12 F_{M-E} ($\eta = 1$: thick solid line, $\eta = 2$: dotted line, $\eta = 3$: thin solid line) as a function of t; $J_x = 1$, $J_y = 3$, $J_z = 2$, $b = 1$, $B = 10$

In Fig. 15 F_{M-P} and F_{M-E} as a function of decoherence phase η are plotted. It is observed that as η increases, both entangled and non-entangled Milburn fidelity increase, but finally they follow their respective plateaus.

7 Conclusions and Discussion

For non-entangled Schrödinger channel, in the absence of decoherence, an increase in the inhomogeneous magnetic field, increases fidelity but its fluctuation periods decrease. An increase of the homogeneous magnetic field for this channel does not have any appreciable effect on the fidelity, only increases slightly. For entangled Schrödinger channel, an increase in the inhomogeneous or homogeneous magnetic field increases the fidelity on the average.

For the non-entangled Milburn channel, an increase of the homogeneous or inhomogeneous magnetic field increases the fidelity. For entangled Milburn channel, an increase of the inhomogeneous magnetic field decreases the fidelity, but an increase of the homogeneous magnetic field increases the latter.
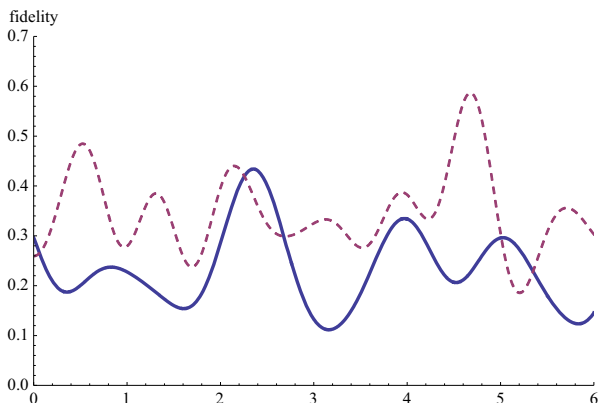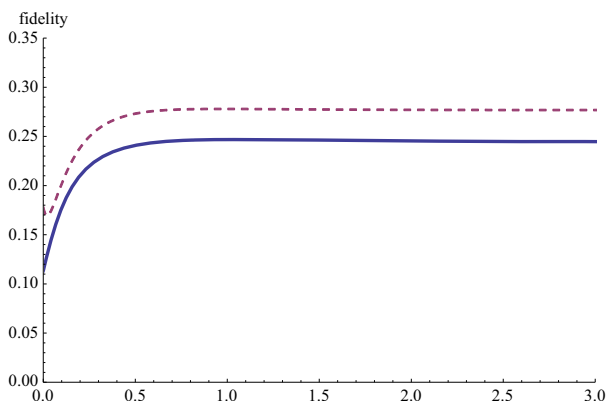

Fig. 13 F_{Sh-P} (solid line) and F_{Sh-E} (dotted line) as a function of t: $J_x = 1$, $J_y = 3$, $J_z = 2$, $b = 1$, $\eta = 1$, $B = 1$
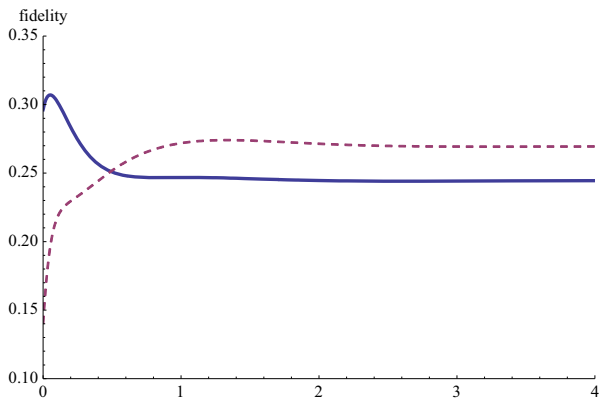
Fig. 14 F_{M-P} (solid line) and F_{M-E} (dotted line) as a function of t: $J_x = 1$, $J_y = 3$, $J_z = 2$, $b = 1$, $\eta = 1$, $B = 1$

We also note an interesting observation regarding the Milburn channel: The fidelity of the entangled Milburn channel increases due to decoherence, while that of the nonentangled channel decreases, due to small decoherence effects; however, for the larger values of the decoherence, the fidelity is not appreciably changed for both entangled and non-entangled channels.

Finally we consider some results obtained in the case of two-qubit teleportation in the presence of the intrinsic decoherence for comparison. In reference (13) it is found that both entangled and non-entangled initial states are appropriate for teleportation and the tuning of the magnetic field can improve the fidelity. We have also observed a similar result regarding our initial-qutrit entangled and non-entangled states in the presence of the magnetic fields. In reference (15) the Dzyaloshinskii–Moriya interaction has also been considered; it is observed that the Dm interaction and both homogeneous and inhomogeneous part of the field can influence the fidelity, depending on the entangled initial state. We observed in our work that for the qutrit-entangled Milburn channel, an increase of the inhomogeneous magnetic field decreases the fidelity, but an increase of the homogeneous magnetic field increases the latter.

Fig. 15 F_{M-P} (solid line) and F_{M-E} (dotted line) as a function of η: $J_x = 1$, $J_y = 3$, $J_z = 2$, $b = 1$, $t = 1$, $B = 1$

Appendix 1

$$\Gamma^0 = \begin{pmatrix} 1 & 0 & 0 \\ 0 & 1 & 0 \\ 0 & 0 & 1 \end{pmatrix}, \tag{25}$$

$$\Gamma^1 = \begin{pmatrix} 0 & 1 & 0 \\ 1 & 0 & 0 \\ 0 & 0 & 0 \end{pmatrix}, \tag{26}$$

$$\Gamma^2 = \begin{pmatrix} 0 & -i & 0 \\ i & 0 & 0 \\ 0 & 0 & 0 \end{pmatrix}, \tag{27}$$

$$\Gamma^3 = \begin{pmatrix} 1 & 0 & 0 \\ 0 & -1 & 0 \\ 0 & 0 & 0 \end{pmatrix}, \tag{28}$$

$$\Gamma^4 = \begin{pmatrix} 0 & 0 & 1 \\ 0 & 0 & 0 \\ 1 & 0 & 0 \end{pmatrix}, \tag{29}$$

$$\Gamma^5 = \begin{pmatrix} 0 & 0 & -i \\ 0 & 0 & 0 \\ i & 0 & 0 \end{pmatrix}, \tag{30}$$

$$\Gamma^6 = \begin{pmatrix} 0 & 0 & 0 \\ 0 & 0 & 1 \\ 0 & 1 & 0 \end{pmatrix}, \tag{31}$$

$$\Gamma^7 = \begin{pmatrix} 0 & 0 & 0 \\ 0 & 0 & -i \\ 0 & i & 0 \end{pmatrix}, \tag{32}$$

$$\Gamma^8 = \frac{1}{\sqrt{3}} \begin{pmatrix} 1 & 0 & 0 \\ 0 & 1 & 0 \\ 0 & 0 & -2 \end{pmatrix}. \tag{33}$$

Appendix 2

$$|\phi^0\rangle = \frac{1}{\sqrt{3}}\left(|2,0\rangle + |1,1\rangle + |0,2\rangle\right) \tag{34}$$

$$|\phi^1\rangle = \frac{1}{\sqrt{3}}\left(|1,0\rangle + |0,1\rangle + |2,2\rangle\right) \tag{35}$$

$$|\phi^2\rangle = \frac{1}{\sqrt{3}}\left(|0,0\rangle + |2,1\rangle + |1,2\rangle\right) \tag{36}$$

$$|\phi^3\rangle = \frac{1}{\sqrt{3}}\left(|2,0\rangle + e^{\frac{2\pi i}{3}}|1,1\rangle + e^{-\frac{2\pi i}{3}}|0,2\rangle\right) \tag{37}$$

$$|\phi^4\rangle = \frac{1}{\sqrt{3}}\left(|1,0\rangle + e^{\frac{2\pi i}{3}}|0,1\rangle + e^{-\frac{2\pi i}{3}}|2,2\rangle\right) \tag{38}$$

$$|\phi^5\rangle = \frac{1}{\sqrt{3}}\left(|0,0\rangle + e^{\frac{2\pi i}{3}}|2,1\rangle + e^{-\frac{2\pi i}{3}}|1,2\rangle\right) \tag{39}$$

$$|\phi^6\rangle = \frac{1}{\sqrt{3}}\left(|2,0\rangle + e^{-\frac{2\pi i}{3}}|1,1\rangle + e^{\frac{2\pi i}{3}}|0,2\rangle\right) \tag{40}$$

$$|\phi^7\rangle = \frac{1}{\sqrt{3}}\left(|1,0\rangle + e^{-\frac{2\pi i}{3}}|0,1\rangle + e^{\frac{2\pi i}{3}}|2,2\rangle\right) \tag{41}$$

$$|\phi^8\rangle = \frac{1}{\sqrt{3}}\left(|0,0\rangle + e^{-\frac{2\pi i}{3}}|2,1\rangle + e^{\frac{2\pi i}{3}}|1,2\rangle\right) \tag{42}$$

References

1. Horodecki, R., Horodecki, P., Horodecki, M., Horodecki, K.: Quantum entanglement. Rev. Mod. Phys. **81**, 865 (2009)
2. Bennett, C.H., Divincenzo, D.P.: Quantuminformation and computation. Nature. **404**, 247–255 (2000)
3. Feynman, R.: Simulating physics with computers. Int. J. Theor. Phys. **21**, 467 (1982)
4. Gisin, N., Thew, R.: Quantum communication. Nat. Photonics. **1**, 165–171 (2007)
5. Loss, D., DiVincenzo, D.P.: Quantum computation with quantum dots. Phys. Rev. A. **57**, 120 (1998)
6. Burkard, G., Loss, D., DiVincenzo, D.P.: Coupled quantum dots as quantum gates. Phys. Rev. B. **59**, 2070 (1999)

7. Mattis, D.C.: The theory of magnetism made simple: an introduction to physical concepts and to some useful mathematical methods. World Scientific, Singapore (2006)
8. Chen, S., Wang, L., Gu, S.-J., Wang, Y.: Fidelity and quantum phase transition for the Heisenberg chain with next-nearest neighbor interaction. Phys. Rev. E. **76**(1–4), 061108 (2007)
9. Ye, Y.: Teleportation via thermally entangled state of a two-qubit Heisenberg XX chain. Phys. Lett. A. **309**(3–4), 215–217 (2003)
10. Li, S.-B., Xu, J.-B.: Magnetic field effects on the optimal fidelity of standard teleportation via the two qubits Heisenberg XX chain in thermal equilibrium. arXiv:quant-ph/0312125 (2004)
11. Yeo, Y., Liu, T., Lu, Y.-E., Yang, Q.-Z.: Quantum teleportation via a two-qubit Heisenberg XY chain— effects of anisotropy and magnetic field. J. Phys. A Math. Gen. **38**(14), 3235 (2005)
12. Hao, X., Zhu, S.: Entanglement teleportation through 1D Heisenberg chain. Phys. Lett. A. **338**(3–5), 175–181 (2005)
13. He, Z., Zuhong, X.Y.Z.: Influence of intrinsic decoherence on quantum teleportation via two-qubit Heisenberg XYZ chain. Phys. Lett. A. **354**, 79–83 (2006)
14. Javad Akhtarshenas, S., Kheirandish, F., Mohammadi, H.: Influence of Dephasing on the Entanglement Teleportation via a two-qubit Heisenberg XYZ system. The European Physical Journal D. **62**(3), 439–447 (2011)
15. Zidan, N.: Quantum teleportation via two-qubit Heisenberg XYZ chain. Can. J. Phys. **92**, 406–411 (2014)
16. Qin, M., Ren, Z.-Z.: Influence of intrinsic decoherence on entanglement teleportation via a Heisenberg XYZ model with different Dzyaloshinskii-Moriya interaction. Quantum Inf. Process. **14**(6), 2055–2066 (2015)
17. Milburn, G.J.: Intrinsic decoherence in quantum mechanics. Phys. Rev. A. **44**(9), 5401–5406 (1991)
18. Guo, J.-L., Xia, Y., Song, H.-S.: Effects of Dzyaloshinski–Moriya anisoyropic antisymmetric interaction on entanglement and teleportation in a two-qubit Heisenberg chain with intrinsic decoherence. Opt. Commun. **281**, 2326–2330 (2008)
19. Delgado, A., Saavedra, C., Retamal, J.C.: Quantum information and entanglement transfer for qutrits. Phys. Lett. A. **370**(1), 22–27 (2007)
20. Mei-Yu, W., Feng-Li, Y.: Probabilistic chain teleportation of a qutrit-state. Commun. Theor. Phys. **54**(2), 263 (2010)
21. Chamoli, A & Bhandari, C. M.: Entanglement teleportation by qutrits. arXiv:quant-ph/0702223 (2007)
22. Jafarpour, M., Naderi, N.: Qutrit teleportation under intrinsic decoherence. International Journal of Quantum Information. **14**(5), 1650028 (2016)
23. Jami, S., Amerian, Z.: Thermal entanglement of a qubit-qutrit chain. IJRAP. **3**(2), 75–84 (2014)
24. Liang, Q., An-Min, W., Xiao-San, M.: Effect of Intrinsic Decoherence of Milburn's Model on Entanglement of Two-Qutrit States. Commun. Theor. Phys. **49**(2), 516–520 (2008)
25. Bowen, G., Bose, S.: Teleportation as a depolarizing quantum channel, relative entropy, and classical capacity. Phys. Rev. Lett. **87**, 267901 (2001)
26. Arvind, K.S.M., Mukunda, N.: A generalized Pancharatnam geometric phase formula for three level quantum systems. J. Phys. A Math. Gen. **30**(7), 2417 (1997)
27. An, N.B.: Teleportation of two-quNit entanglement: Exploiting local resources. Phys. Lett. A. **9–14**, 341 (2005)
28. Jozsa, R.: Fidelity for mixed quantum states. J. Mod. Opt. **41**(12), 2315–2323 (1994)